Combinational Rogowski Coil with Enhanced DC Measurement Capability for Double Pulse Test Applications

Sadia Binte Sohid
Min H. Kao Department of Electrical Engineering and Computer Science
University of Tennessee Knoxville
Knoxville, United States
ssohid@vols.utk.edu

Han (Helen) Cui
Min H. Kao Department of Electrical Engineering and Computer Science
University of Tennessee Knoxville
Knoxville, United States
helencui@utk.edu

Wen Zhang
Min H. Kao Department of Electrical Engineering and Computer Science
University of Tennessee Knoxville
Knoxville, United States
wen.zhang@utk.edu

Fred Wang
Min H. Kao Department of Electrical Engineering and Computer Science
University of Tennessee Knoxville
Knoxville, United States
fred.wang@utk.edu

Bernhard Holzinger
Keysight Technologies
Boblingen, Germany
bernhard_holzinger@keysight.com

2022 IEEE Energy Conversion Congress and Exposition (ECCE) | 978-1-7281-9387-8/22/$31.00 ©2022 IEEE | DOI: 10.1109/ECCE50734.2022.9947541

***Abstract*— The DC measurement capability and high-frequency bandwidth are vital aspects for current sensors to accurately capture the switching current behavior of wide bandgap devices. However, typical Rogowski coil (RC) current sensors lack DC sensing capability resulting in inaccurate low-frequency measurement results. This paper presents a concept of combinational RC with improved DC measurement capability without intruding the power loop area for double pulse test (DPT) systems. The DC current sensor and the RC are placed at different locations to capture the low-frequency and high-frequency switching current, respectively. An analog adder circuit is used to combine the two sensing results, thereby extending the measurement bandwidth of the RC without increasing the insertion parasitic inductance. The frequency-domain measurement of the combinational RC with DC sensors verifies the extended DC measurement bandwidth. In the paper, the switching current measured from a half-bridge SiC power module under DPT has been used as an example to demonstrate the enhanced measurement capability of this combinational RC avoiding an increase of extra parasitic.**

Keywords—Combinational RC, DC measurement, Hall Sensor, double pulse test, power loop.

I. INTRODUCTION

The wide-bandgap (WBG) devices, such as SiC and GaN, has high switching capabilities, which causes steeper current slopes. The transient switching behavior of these devices is sensitive to the power loop inductance [1]. A smaller power loop area provides a lower stray inductance effect in the transient behavior of these devices. Consequently, using a current sensor with low insertion inductance is essential. Also, a high frequency bandwidth current sensor is required to precisely capture the fast switching transition of the commutation current. Several high bandwidth current sensors, such as resistive current shunt and current transformers, are commercially available to measure the fast switching current. Though resistive current shunt has a high frequency bandwidth of several GHz, the large size introduces large stray inductance in the measurement path [2]. Also, in the application of high current with low voltage, it reduces its efficiency for high power consumption. Another current sensing technology, the current transformer, is widely used for its no power consumption and high bandwidth of several MHz (250 MHz) [3]. However, the core material used in this sensing method limits the DC and low frequency measurement [3]. The Rogowski coil (RC) is relatively non-invasive and has low insertion inductance compared with other current probes [4]. The air-core used in this probe eliminates the limitations of using the core material.

The improvement of low freqeuncy bandwidth or the DC measurement capability of a current sensor is as crucial as high frequency bandwidth because the commutation current waveform in power electronic circuits is similar to a pulsed current source, consisting of steep slopes, high-frequency ripples, and DC components. The insufficient DC measurement capability of a current probe creates an offset from the real DC value or a misalignment of the commutation current waveform [5], [6]. Therefore, in this paper, we emphasize on improving the low freqeuncy bandwidth of the combinational Rogowski Coil.

A recently developed PCB-based combinational RC prototype is shown in Fig. 1. This combinational RC has improved the high bandwidth (HBW) to 250 MHz (Fig. 2) with a small size by adding shielding layers [7]. The circumference of this coil is 25 mm (major radius (R) = 2 mm), which is much smaller compared to the conventional ones. The coil uses copper shielding layers to cover the windings from the outside, as shown in Fig 1(a). The parasitic capacitance between these shielding layers and coil windings exhibits a self-integrating

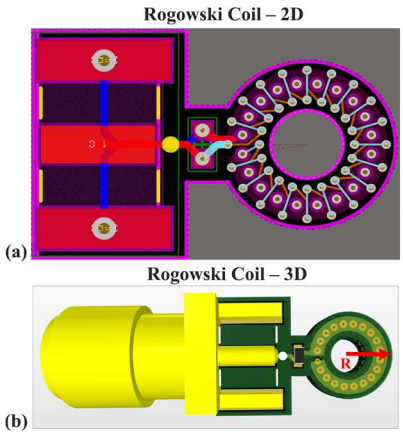

Fig. 1. A PCB based Combinational Rogowski Coil in (a) 2D, and (b) 3D view.

region (7 MHz ~ 250 MHz) for the combinational RC [7], which extends the high frequency region of the coil. However, the low frequency bandwidth is compromised to 20 kHz, making it hard to capture the DC components of the commutation current during device switching transients. To enhance the DC measurement capability of this RC, we propose to add a DC magnetic sensor with the RC based on the 'HOKA' principle to obtain a wide frequency bandwidth range [5]. The 'HOKA' principle refers to the combination of two different sensor outputs. One comes from a DC sensor, and the other output must be the derivative of the primary current (di/dt). Following the 'HOKA' principle, a transducer consists of a planar current transformer, and a hall element sensor was proposed in [6]. The hall element was implemented in the air-gap region of the current transformer, so the limitation arises to balance the size of the air-gap and the hall element. Another type is the multiple TMR sensors mounted on top of the Rogowski coil [8]. A co-axial housing has been used to hold the Rogowski coil and the signal processing unit. Therefore, this implemention would increase the power loop inductance [9]. This paper discusses an alternative method to incorporate the DC sensor with the RC without introducing any extra parasitic in the power loop region of the double pulse test circuit to enhance the DC measurement

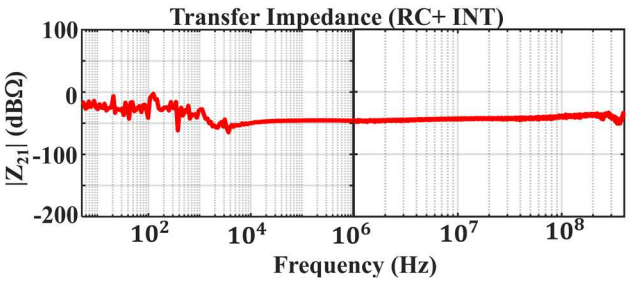

Fig. 2. The transfer impedance (Z_{21}) of the Rogowski coil and integrator circuit measured using the Network Analyzer.

of the combinational RC sensor. The experimental results verified the enhanced DC measurement ability of the RC while placing the DC sensor outside of the power loop region of the DPT board.

II. Methodology

The 'HOKA' principle [5] is a method that utilizes two isolated current sensors (DC magnetic sensor and Rogowski coil) to measure the low and high frequency components of the current waveform separately. Both sensors must have,

(a) similar sensitivity ($Z_{21} = \frac{V}{I}$), and

(b) an adjusted cut-off frequency (F_c)

to obtain a flat gain curve over a wide frequency range. Fig. 3 illustrates the 'HOKA' method that combines two sensors and provides a flat gain curve for the current probe. The main focus of this paper is to discuss about an alternative method to enhance the DC measurement capability of the RC in the double pulse

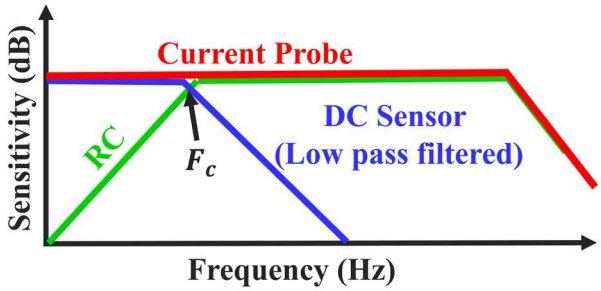

Fig. 3. The illustration of 'HOKA' method [5].

test (DPT) circuit application. The most significant part is to place the DC sensor outside of the power loop region to capture the DC or low-frequency components of the current waveform. The reason behind placing the RC coil and the DC sensor at two separate locations of the DPT circuit has been explained in detail in this section.

In the applications of the DPT circuit, the dc and ac components in the switching current can actually be decoupled. The dc link capacitor (C_1) mainly supplies the dc component of the switching current, while the ac component by the dc link capacitor and decoupling capacitor together [10]. Therefore, the DC sensor can be separated from the Rogowski coil location to avoid introducing extra stray inductance in the power loop. Mostly, the RC coil is placed at the source (S) terminal of the lower device (inside the power loop) to measure the switching current. Fig. 4(a) shows a double pulse test circuit with arrows indicating the DC (I_{Low}) and AC (I_{Decap}) components of the switching current (I_{SW}) of the device under test (DUT). The time domain waveform indicating I_{Low}, I_{Decap}, and I_{SW} are shown in Fig. 4(b). The FFT analysis of I_{Low} and I_{SW} shows that the low frequency components of the switching current (I_{SW}) coincides with the low frequency components of I_{Low} (Fig. 4(c)), which validates the concept that the dc component can be measured separately outside the power loop. The DC magnetic sensor can be placed between the DC bulky capacitors (C_1) and the decoupling capacitors (C_{in2}) (see Fig. 4(a)), which will capture the DC components of I_{SW}. In contrast, the combinational RC set at the source(S) terminal of the DUT (see Fig. 4(a)) will measure the high-frequency components. These two results added together yields the complete spectrum of the switching current I_{SW}. Hence, the main advantage of this method is that the DC measurement capability is enhanced for the combinational

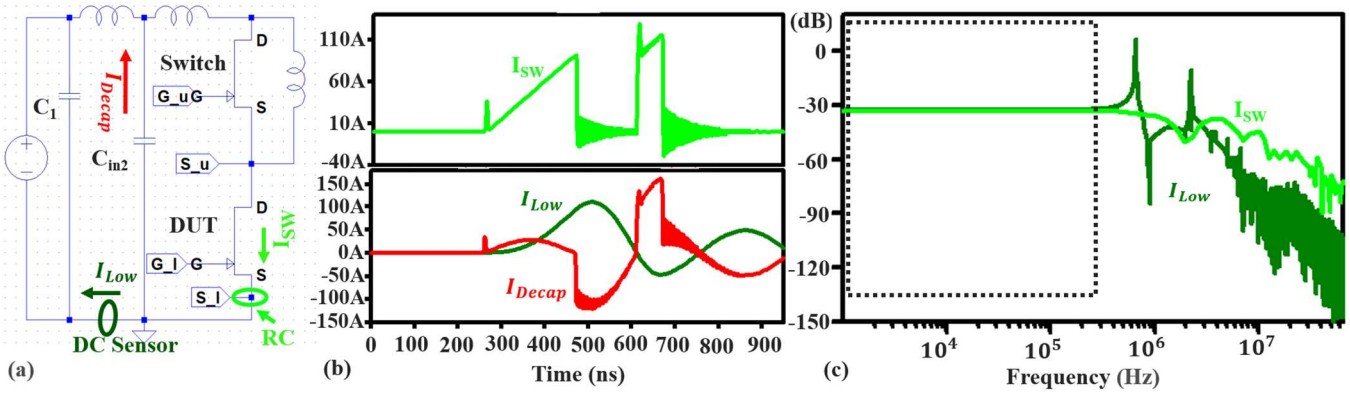

Fig. 4. (a) The double pulse test circuit, (b) the time domain waveforms of I_{Low}, I_{Decap}, and the I_{SW}, and (c) the frequency spectrum of the I_{Low} and the I_{SW} waveforms of the DPT circuit showing overlapped low frequency components.

RC without inserting extra components into the power loop region of the DPT system.

In the following section III, we will represent the simulation results of the entire probe system, which follows the 'HOKA' principle. Then, all the experimental results both in frequency domain and time-domain will be demonstrated in section IV to verify the proposed method.

III. Simulation Results

A simulation model (Fig. 5) has been built to realize the frequency-domain response of the combined RC and DC magnetic sensor. The model for the RC has been developed from its real physical prototype using Matlab algorithm. The DC sensor acts as a low-pass filter [6]; therefore, it has been modeled by a RC (R1 & C1) filter and a voltage divider (R2 & R3) circuit, which denote the cut-off frequency and the sensitivity of the sensor (Fig. 5) respectively. The selected DC sensor is a Hall sensor (LESR 50 NP) with a frequency bandwidth of 300 kHz and a sensitivity of 12.5 mV/A [11], matching the sensitivity with the combinational RC (Z_{21}= 10 mV/A). As mentioned in the methodology section, an adjusted the cut-off frequency (F_c) is required for both sensors to obtain a wide bandwidth flat gain curve. The Hall sensor will only capture the current signal that ranges from the DC ~ Fc. On the other hand, the (RC+INT) will capture the signal ranging from the Fc ~ HBW. Additional high (CH & RH) and low pass (CL & RL) filters are required to tune the cut-off frequency (F_c), and filter out increased noise. The

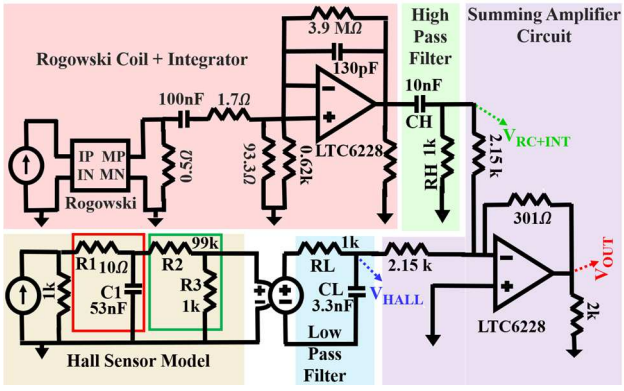

Fig. 5. The simulation model of the current measurement system with Rogowski coil and Hall sensor.

intrinsic noise of the op-amp (LTC6228) used in the integrator (INT) circuit limits the lower bandwidth of the combinational RC below 20 kHz (Fig. 2). It is better to keep a margin in the selection of the cut-off frequency (Fc) of the filters to avoid the inclusion of the op-amp noise in the system. Therefore, the cut-off frequency of both filters is chosen to be 45 kHz for both sensors (Hall & RC) instead of 20 kHz.

Mathematically, the cut-off frequency of the low pass filter (RL = 1 kΩ & CL = 3.3nF),

$$F_c = \frac{1}{2\pi * RL * CL} = 48\ kHz \quad (1)$$

The high pass filter corner frequency should be 48 kHz if RH = 10 kΩ & CH = 330pF.

$$F_c = \frac{1}{2\pi * RH * CH} = 48\ kHz \quad (2)$$

It should be noted that the paralleling effect of RH with other nearby resistors shifts the corner frequency at a higher value than 48 kHz. Hence, the RH and CH value has been tuned to match the cut-off frequency (F_c) at 48 kHz. The analog adder circuit

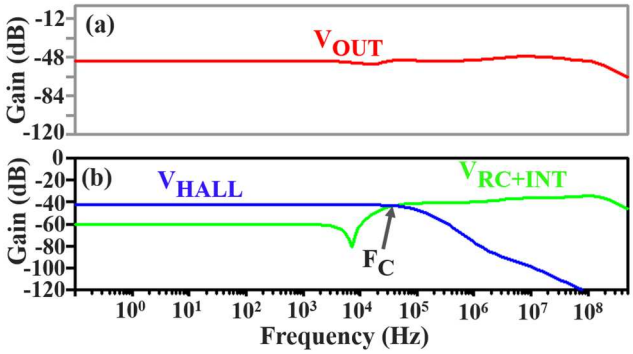

Fig. 6. The simulated waveforms for (b) V_{OUT} (c)V_{HALL} and V_{RC+INT} in the circuit shown in Fig. 5.

combines both Hall and RC sensor signals, resulting in a flat gain curve (V_{OUT}) (Fig. 6), which means a wide-bandwidth sensor. The gain of the adder circuit is -16dB. The flat gain curve (Fig. 6) verifies the 'HOKA' principle of the system.

IV. Experimental Verification

In this section, we will first demonstrate the frequency response of the prototype to verify the simulation result shown in Fig. 6. The gain curve will illustrate the current capturing capability of the entire system. Secondly, the sensors will be implemented in the DPT circuit, as described in Fig. 4(a). Finally, the results verify the DC improvement of the Rogowski coil without introducing extra parasitic in the power loop of a DPT circuit.

A. Frequency Domain Response

A prototype is built to analyze the frequency response of the Rogowski Coil, the Hall sensor (LESR 50-NP), and the adder circuit. The Network Analyzer (E5061B – 3L5) has been utilized to measure both the high-frequency and the low-frequency response of the system. The S- parameter test port can measure in the high frequency range of 300 kHz ~ 3 GHz, and the gain-phase test port is used to measure relatively low frequency from 5Hz ~ 30MHz.

At first, the transfer impedance ($Z_{21} = \frac{V}{I}$) of the hall sensor and RC are measured separately. Fig. 7(a) shows the transfer impedance curve (low frequency measurement) of the hall sensor. The sensitivity is measured to be 12.5 mV/A (-38dB), which matches the datasheet value. As discussed above, the low

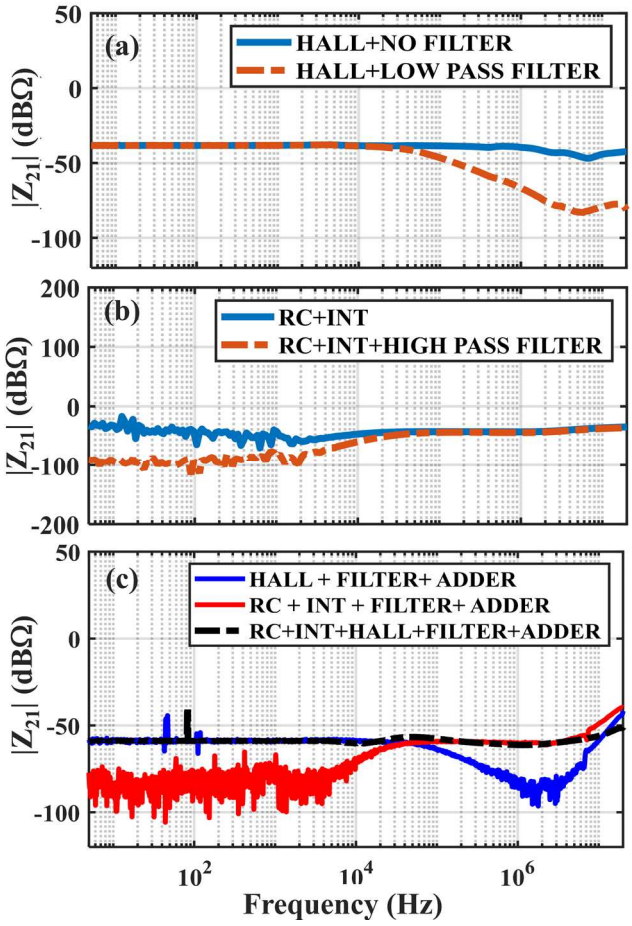

Fig. 7. The transfer impedances of (a) HALL sensor w/o the low pass filter; (b) Rogowski coil with integrator and high pass filter, and (c) the entire system.

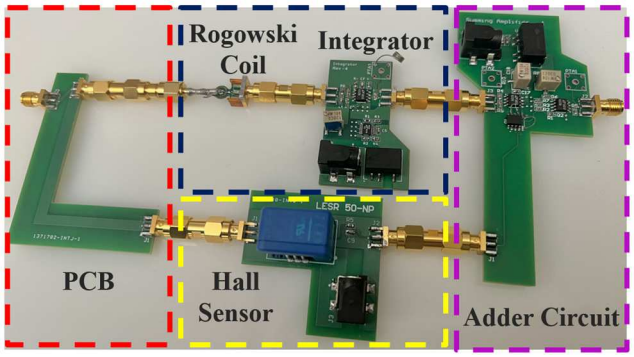

Fig. 8. Prototype system used to verify the HOKA principle in the frequency domain.

pass filter is added after the hall sensor to adjust the cut-off frequency (F_c) and reduce the high-frequency noise. The RC+INT shows 10 mV/A (- 40dB) sensitivity from the transfer impedance (Fig. 2). The high pass filter reduces the low frequency noise of the RC+INT (Fig. 7(b)), and also used to adjust the F_c value. Both the filters cut-off frequency is adjusted to 45 kHz as discussed in the simulation section (Fig. 6).

To combine both sensors and verify the 'HOKA' principle experimentally, a PCB (Fig. 8) is used as a fixture to connect the RC and the Hall sensor in series such that the same current from the Network Analyzer is measured by both the RC and the Hall sensor. Then, the outputs of both sensors are sent to the input of the adder circuit. The black curve in Fig. 7(c) represents a flat gain curve from a low frequency of 5 Hz to 20MHz. That means the DC measurement capability is enhanced for the RC+INT, which was limited to 20 kHz (Fig. 2). The flat gain curve obtained experimentally, which is shown in Fig. 7(c), matches with the simulation result of Fig. 6.

B. Time Domain Response

To measure the response of the probe prototype in the time domain, the sensors are used in a DPT circuit. The position of the sensors and the connections are shown in Fig. 9. The

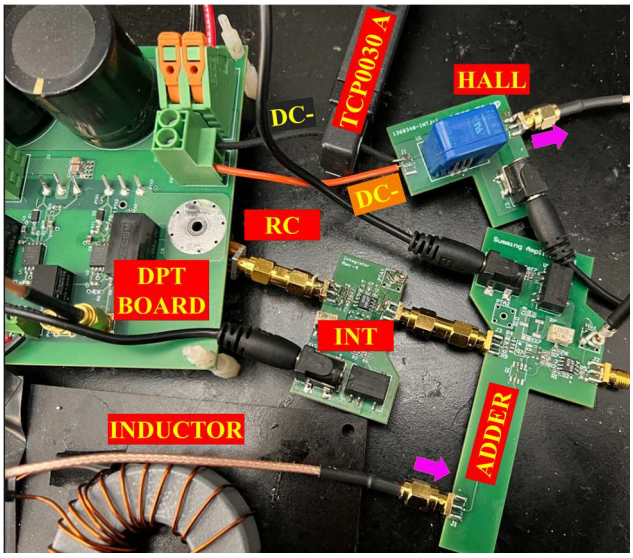

Fig. 9. The implementation of the current measurement in a double-pulse test circuit for a half-bridge SiC module.

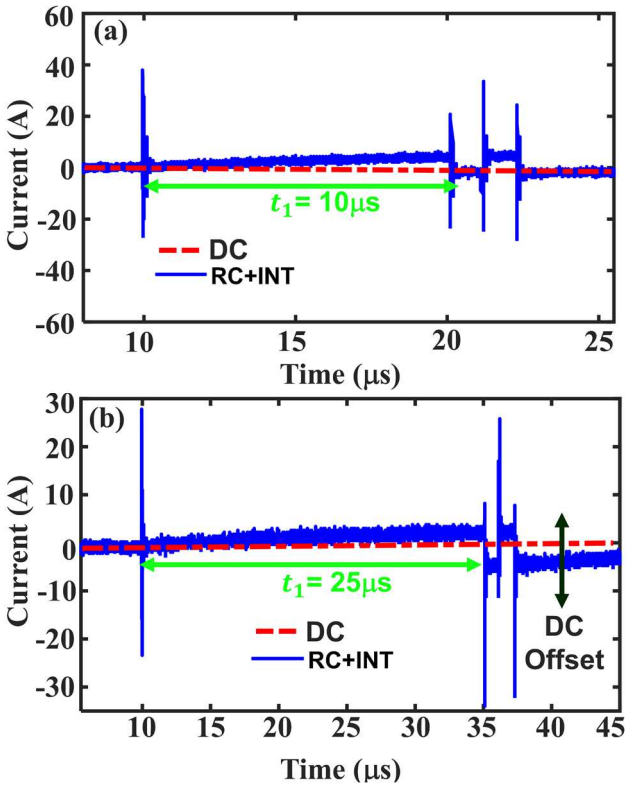

Fig. 10. The output of RC+INT when (a) t_1 = 10μs and (b) t_1 = 25μs under an operating voltage of 400V and load inductance of 400μH showing the DC offset issue.

resistive shunt footprint is shorted with a wire that is fed through the RC. The hall sensor is placed between the DC- terminals, so that the current flows through the low resistance path of the hall sensor. Due to the hall effect, a voltage will be generated at the output of the hall sensor. Both the (RC+INT) and Hall (LESR 50-NP) sensor are connected to the input terminals of the adder circuit using SMA connectors. The load inductor that is used in the DPT circuit is 400μH. All the results are discussed in the following sub-sections.

B(1). (RC+INT) Output

The required bandwidth of a probe is measured by the transition time (t_r) [12]. The required bandwidth (F_{knee}) can be determined by,

$$F_{knee} = \frac{0.5}{t_r} \tag{3}$$

To measure the switching current waveform, the required bandwidth must fall in the flat gain region. The relation between the primary current and output voltage must be linear, thus always a constant mutual inductance (Z_{21} = M) between the coil and conductive wire. The RC+INT output is demonstrated with two different pulse widths (t_1 = 10μs & t_1 = 25μs) in the DPT. The reason behind analyzing two different pulses is to identify the real disadvantage of the low frequency bandwidth of the RC. The difference between Fig. 10(a) and Fig. 10(b) is the DC level shift. When the pulse width is t_1 = 25 us, a DC offset is observed. This is because the corner frequency of RC+INT (48 kHz) is

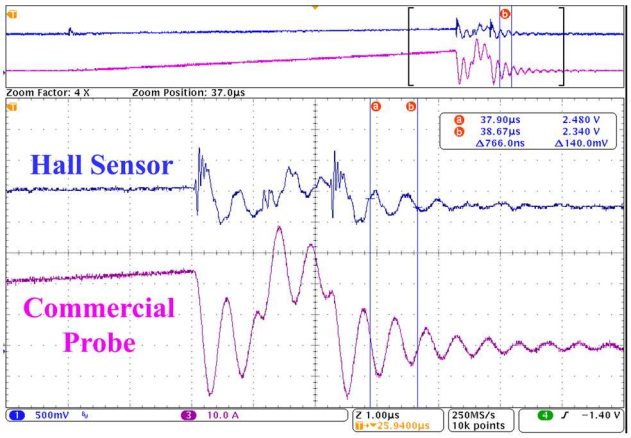

Fig. 11. The measured current using Hall sensor and the commercial probe.

higher than the required bandwidth to measure the current at t_1 = 25us ($F_{25\mu s}$ = 20 kHz, $F_{10\mu s}$ = 50 kHz). As the (RC+INT) sensor has limited low frequency measurement capability, the higher pulse width waveform starts to create more DC offset. This proves the necessity of improving the DC measurement of the Rogowski coil. Enhancing the DC measurement of the Rogowski coil will remove the DC offset issue.

B(2). Hall Sensor Output

The position of the Hall sensor has been depicted in Fig. 4(a). A commercial current probe TCP0030 A (50A, 120 MHz) is also placed at the same location to verify and compare the measured current from the Hall sensor (LESR-50NP). The measured waveforms from the Hall sensor and the commercial current probe are shown in Fig. 11. Other than the low-frequency current captured by the Hall sensor, some high-frequency ripples also appear in the waveform. The amount of high frequency

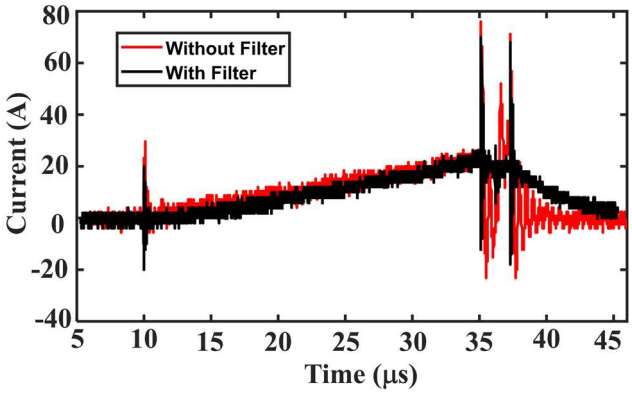

Fig. 12. The low pass filter eliminated the high frequency ripples from the Hall sensor output.

ripples that leaks into the low frequency path depends on the value of the decoupling capacitor, but they won't impact the result since they will be filtered out by the low pass filter added following the DC sensor, which is shown in Fig. 12.

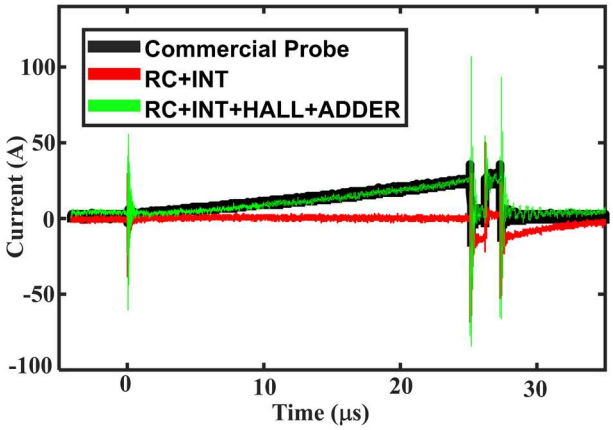

Fig. 13. Improved DC measurement capability after adding the DC sensor showing the DC offset issue is removed from the Rogowski coil and integrator output.

B(3). The (RC+INT+HALL+ADDER) Output

The complete system consists of the Rogowski coil, integrator, Hall sensor, and the adder circuit. The adder circuit will combine the low frequency and high frequency spectrums of the current waveform. The DC measurement capability of the system has been enhanced, which is verified by the frequency response (Fig. 7(c)). As a result, the DC level shift encountered from the (RC+INT) circuit has been eliminated. The sensitivity of the entire system is 1.25mV/A (-58 dB). Fig. 13 verifies the DC enhancement of the Rogowski coil by removing the DC level shift. Also, it proves that, the DC measurement capability of the system can be improved without intruding the power loop inductance in the DPT circuit. However, compared to the commercial current probe, large spikes are observed during the transition time instants, which is caused by the gain increase of the hall sensor at high frequency. The overall performance and the further improvement to take for the probe are elaborated in the following sub-section.

B(4). The High Frequency Distortion

Since the steep slopes in the current waveforms correspond to the high frequency components, the gain curve of the probe must be flat in the high frequency range to measure those steep slopes correctly. However, the addition of the Hall sensor and adder circuit introduces large noise in the high-frequency range and creates a non-flat distorted gain curve of the probe system at high frequency, which give rise to the large spikes in the switching current.

As shown in Fig. 14(a), the Hall sensor (LESR-50NP) noise ramps up at approximately 20MHz even with a second-order low-pass filter added, distorting the flat gain curve. An alternative DC sensor with low noise at a high frequency will improve the high frequency bandwidth of the probe system.

On the other hand, the op-amp (LTC6228) used in the adder circuit is selected to take advantage of the ultra-low voltage noise at the low frequency range and rail-to-rail output [13]. However, its gain curve peaks around 50 MHz as shown in Fig. 14(b) that also undermines the high bandwidth of the probe system. Choosing a better op-amp or an alternative method to

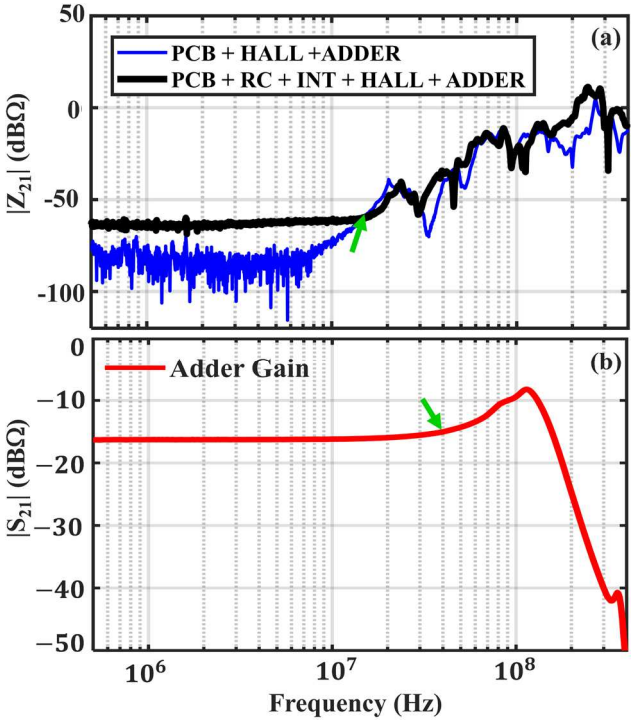

Fig. 14. (a) Response of the probe system showing noise from the Hall sensor; (b) increased gain of the adder circuit in the high frequency range.

sum the output of the two sensors should be studied to maintain the high frequency bandwidth of the probe system. These are the tasks under investigation and will be reported in subsequent publications.

V. Conclusion

The combinational RC has achieved a high frequency bandwidth of 250 MHz thanks to its self-integrating property. However, the low-frequency bandwidth of the RC is limited to 20 kHz that compromises the low-frequency measurement capability of the RC. A DC sensor (Hall-effect sensor) is combined with the RC to enhance the low-frequency measurement capability. This paper implements the combination of these two sensors to achieve a flat gain over the wide frequency range without introducing any parasitic inductance in the power loop zone of the DPT circuit. The RC coil is placed inside the power loop, and the Hall sensor outside the power loop. The main advantage of this method is that there is no increase in the power loop parasitic with the inclusion of the Hall sensor in the DPT application. Experimental results on a SiC power module DPT system of both the frequency and time-domain response validate the concept and show the dc current offset is removed from the RC measurement results. Future work includes eliminating the noises at high-frequency range from the DC sensor and adder circuit to maintain the high-frequency bandwidth of the combinational RC.

VI. Acknowledgement

This work is supported by the Engineering Research Center Program of the National Science Foundation and the Department of Energy under NSF Award Number EEC

1041877 and the CURENT Industry Partnership Program with Keysight Technologies.

VII. REFERENCES

[1] Z. Huang *et al.*, "A novel low inductive 3D SiC power module based on hybrid packaging and integration method," in *2017 IEEE Energy Conversion Congress and Exposition (ECCE)*, 2017: IEEE, pp. 3995-4002.

[2] C. Xiao, L. Zhao, T. Asada, W. Odendaal, and J. Van Wyk, "An overview of integratable current sensor technologies," in *38th IAS Annual Meeting on Conference Record of the Industry Applications Conference, 2003.*, 2003, vol. 2: IEEE, pp. 1251-1258.

[3] F. Costa, E. Labouré, F. Forest, and C. Gautier, "Wide bandwidth, large AC current probe for power electronics and EMI measurements," *IEEE Transactions on Industrial Electronics,* vol. 44, no. 4, pp. 502-511, 1997.

[4] M. H. Samimi, A. Mahari, M. A. Farahnakian, and H. Mohseni, "The Rogowski coil principles and applications: A review," *IEEE Sensors Journal,* vol. 15, no. 2, pp. 651-658, 2014.

[5] N. Karrer and P. Hofer-Noser, "A new current measuring principle for power electronic applications," in *11th International Symposium on Power Semiconductor Devices and ICs. ISPSD'99 Proceedings (Cat. No. 99CH36312)*, 1999: IEEE, pp. 279-282.

[6] P. Poulichet, F. Costa, and É. Labouré, "A new high-current large-bandwidth DC active current probe for power electronics measurements," *IEEE Transactions on Industrial Electronics,* vol. 52, no. 1, pp. 243-254, 2005.

[7] W. Zhang, S. B. Sohid, F. Wang, H. Cui, and B. Holzinger, "High-bandwidth combinational Rogowski Coil for SiC MOSFET power module," *IEEE Transactions on Power Electronics,* vol. 37, no. 4, pp. 4397-4405, 2021.

[8] N. Tröster, T. Eisenhardt, M. Zehelein, J. Wölfle, J. Ruthardt, and J. Roth-Stielow, "Improvements of a coaxial current sensor with a wide bandwidth based on the HOKA principle," in *2018 20th European Conference on Power Electronics and Applications (EPE'18 ECCE Europe)*, 2018: IEEE, pp. P. 1-P. 9.

[9] N. Tröster, B. Dominković, J. Wölfle, M. Fischer, and J. Roth-Stielow, "Wide bandwidth current probe for power electronics using tunneling magnetoresistance sensors," in *2017 IEEE 12th International Conference on Power Electronics and Drive Systems (PEDS)*, 2017: IEEE, pp. 35-40.

[10] Z. Chen, D. Boroyevich, P. Mattavelli, and K. Ngo, "A frequency-domain study on the effect of DC-link decoupling capacitors," in *2013 IEEE Energy Conversion Congress and Exposition*, 2013: IEEE, pp. 1886-1893.

[11] "Hall Effect Sensor, LESR-50NP," 2022. [Online]. Available: https://www.lem.com/en/lesr-50np.

[12] "Understanding Bandwidth Requirements When Measuring Switching Characteristics," 2021. [Online]. Available: https://eepower.com/technical-articles/understanding-bandwidth-requirements-when-measuring-switching-characteristics-in-power-electronic-applications/.

[13] "Low Distortion Rail-to-Rail Output Op Amps with Shutdown, LTC6228," 2022. [Online]. Available: https://www.analog.com/media/en/technical-documentation/data-sheets/ltc6228-6229.pdf.